

Heterobi- and -trimetallic Ion Pairs of Zirconocene-Based Ioselective Olefin Polymerization Catalysts with AlMe₃**

Gabriel Theurkauff, Arnaud Bondon, Vincent Dorcet, Jean-François Carpentier,* and Evgueni Kirillov*

Abstract: The reactivity towards AlMe₃ of discrete cationic *ansa*-zirconocenes **2a,b** that are ubiquitously used in ioselective propylene polymerization and based on $[(\text{Ph}(\text{H})\text{C}(3,6\text{-}t\text{Bu}_2\text{-Flu})(3\text{-}t\text{Bu}\text{-}5\text{-Et}\text{-Cp})\text{ZrMe}_2)]\{\text{Cp}\text{-Flu}\}$ and $\text{rac}\text{-}[(\text{Me}_2\text{Si}(2\text{-Me}\text{-}4\text{-Ph}\text{-Ind})_2)\text{ZrMe}_2]\{\text{SBI}\}$ was scrutinized. The first example of a structurally characterized Group 4 metallocene AlMe₃ adduct (**3b**) is reported. In the presence of excess AlMe₃, the {SBI}-based AlMe₃ adduct **3b** undergoes a slow decomposition via C–H activation in a bridging methyl unit to yield a new species (**4b**) with a trimetallic $\{\text{Zr}(\mu\text{-CH}_2)(\mu\text{-Me})\text{AlMe}(\mu\text{-Me})\text{AlMe}_2\}$ core. EXSY NMR data for the process **2b** ⇌ **3b** → **4b** suggest very rapid and reversible binding of an additional AlMe₃ molecule onto AlMe₃ adduct **3b**. The resulting heterotrimetallic species intermediates exchange of methyl groups between different metal centers and slowly undergoes the C–H activation reaction towards **4b**.

Heterobimetallic ion pairs of the type $[(\text{LX})_2\text{M}(\mu\text{-R})\text{AlR}_2]^+[\text{A}]^-$ (where $\{\text{LX}\}_2\text{M}$ = Group 4 metallocene-type core with R = alkyl; $[\text{A}]^-$ = counteranion, such as $[\text{MeMAO}]^-$, $[\text{B}(\text{C}_6\text{F}_5)_4]^-$) are the cornerstone of modern olefin transformation processes, as they are recognized as dormant species and precursors of chain transfer in polymerization^[1,2] and essential intermediates in carboalumination reactions.^[3] Dissociation of weakly coordinated AlR₃ in the heterobimetallic ion

pair, releasing a catalytically active metallocenium alkyl cation in a bare or solvated form, is considered as a prerequisite step preceding olefin coordination. In general, the stability and reactivity of these heterobimetallic species strongly depend on the nature of the counteranion and ligand and the amount of AlR₃. Though robust heterobimetallic metallocene complexes of the type $[(\text{LX})_2\text{M}(\mu\text{-Me})_2\text{AlMe}_2]^+[\text{B}(\text{C}_6\text{F}_5)_4]^-$ ^[4,5] and $[(\text{LX})_2\text{M}(\mu\text{-Me})_2\text{AlMe}_2]^+[\text{MeMAO}]^-$ ^[6,7] were documented, the post-metallocene heterobimetallic $[\text{Ti}(\text{N}t\text{Bu})(\text{Me}_3[9]\text{aneN}_3)(\mu\text{-Me})_2\text{AlMe}_2]^+[\text{B}(\text{C}_6\text{F}_5)_4]^-$ is, to our knowledge, the only example of a crystallographically characterized Group 4 metal AlMe₃ adduct reported to date.^[8,9] Also, much of the reactivity of these species remains to be learnt, as revealed by recent studies.^[10] Herein we report the reactivity of industrially relevant ioselective {Cp/Flu}- and {SBI}-based *ansa*-zirconocenes towards AlMe₃. The first solid-state structure of a metallocene AlMe₃ adduct, and a complex dynamic process of exchange of methyl groups mediated by formation of a heterotrimetallic bis(AlMe₃) adduct, which eventually results in a unique C–H activation product that was only putative so far, are unveiled.

Treatment of dimethyl complexes $[(\text{Ph}(\text{H})\text{C}(3,6\text{-}t\text{Bu}_2\text{-Flu})(3\text{-}t\text{Bu}\text{-}5\text{-Et}\text{-Cp})\text{ZrMe}_2]$ (**1a**; “{Cp-Flu}”) and $\text{rac}\text{-}[(\text{Me}_2\text{Si}(2\text{-Me}\text{-}4\text{-Ph}\text{-Ind})_2)\text{ZrMe}_2]$ (**1b**; “{SBI}”) with 1 equiv of $[\text{Ph}_3\text{C}]^+[\text{B}(\text{C}_6\text{F}_5)_4]^-$ in a $[\text{D}_8]$ toluene/*o*-F₂-benzene mixture (8:2 v/v)^[11] at room temperature, followed by addition of 2–14 equiv of AlMe₃,^[12] resulted in the immediate and clean formation of the deep-blue and deep-red cationic bimetallic adducts **3a** and **3b**, respectively (Scheme 1).

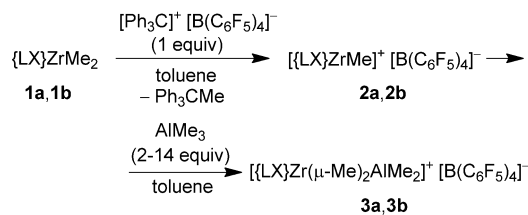
Solution NMR spectroscopic data were acquired immediately on freshly prepared samples. The room-temperature ¹H and ¹³C NMR spectra indicated a C₁ symmetry for **3a** and an average C₂ symmetry on the NMR timescale for **3b** (Supporting Information, Figures S7, S9 and S11, S12). The characteristic hydrogen atoms of the terminal AlMe₂ and bridging Zr(μ-Me)₂Al groups featured high-field chemical shifts: δ = –0.55, –0.66 ppm and –1.18, –1.31 ppm, respectively, for **3a**; δ = –1.55 and –1.24 ppm, respectively, for **3b**.

[*] Dr. G. Theurkauff, Dr. V. Dorcet, Prof. Dr. J.-F. Carpentier, Dr. E. Kirillov
 Organometallics: Materials and Catalysis Laboratories
 UMR 6226 CNRS-Université de Rennes 1
 Institut des Sciences Chimiques de Rennes
 35042 Rennes Cedex (France)
 E-mail: jean-francois.carpentier@univ-rennes1.fr
 evgueni.kirillov@univ-rennes1.fr

Dr. A. Bondon
 Ingénierie Chimique et Molécules pour le Vivant
 UMR 6226 CNRS-Université de Rennes 1
 Institut des Sciences Chimiques de Rennes (France)
 Dr. V. Dorcet
 Centre de diffraction X
 Institut des Sciences Chimiques de Rennes (France)

[**] This work was financially supported by Total Raffinage-Chimie (grant to G.T.). We thank Dr. J.-M. Brusson, Dr. O. Miserque, Dr. A. Vanthomme, and Dr. A. Welle (Total research) for fruitful discussions. C. Orione (CRMPO, UR1) is gratefully acknowledged for technical assistance in PGSE experiments. We are grateful to Dr. T. Roisnel and Dr. L. Toupet for assistance regarding X-ray structural studies. We thank S. Boyer (London Metropolitan University) for elemental analyses.

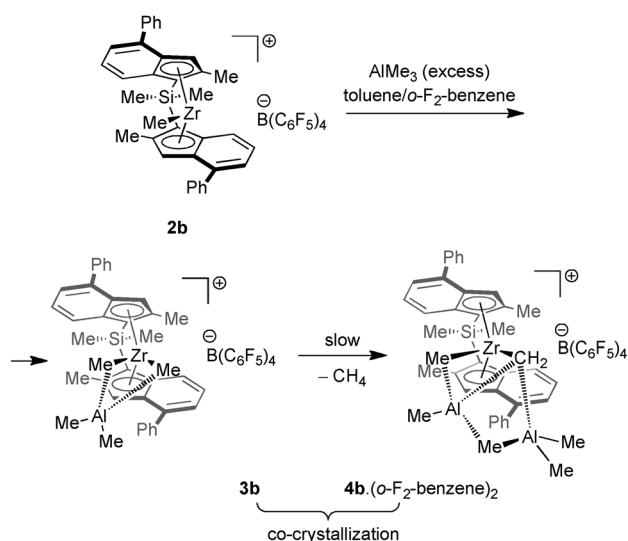
Supporting information for this article is available on the WWW under <http://dx.doi.org/10.1002/anie.201501967>.



Scheme 1. Generation of AlMe₃ adducts **3a** and **3b**.

The PGSE-derived translation diffusion coefficients for **3a** and **3b** ($D_1 = 3.84(6) \times 10^{-10}$ (at 28 mM) and $5.35(6) \times 10^{-10} \text{ m}^2 \text{ s}^{-1}$ (at 10 mM), respectively),^[13] hydrodynamic radii ($r_H = 9.02$ and 7.72 \AA , respectively) and the aggregation number values calculated therefrom ($N = 1.04$ and 0.92 , respectively), were all consistent with the monomeric nature of these species in solution.

All attempts to grow crystals of **3a** failed so far. However, red single crystals were reproducibly obtained and eventually isolated in 30% yield upon storing $[\text{D}_8]\text{toluene}/o\text{-F}_2\text{-benzene}$ solutions of **3b** at -30°C or at room temperature. The X-ray crystallography studies performed on two different batches of such crystals that were obtained in independent experiments revealed their strict identity in terms of crystallographic parameters and composition (see the Supporting Information for details). In fact, two different species co-crystallize together as 1:1 mixed crystals of the expected heterobimetallic complex **3b** and the monocationic heterotrimetallic methylene species **4b** ($o\text{-F}_2\text{-benzene}$)₂ (Scheme 2). The latter complex **4b** is the product of a C–H activation reaction involving one of the two $\{\text{Zr}(\mu\text{-Me})_2\text{Al}\}$ bridging methyl groups in **3b** and an additional AlMe_3 molecule, and implying concomitant release of a molecule of CH_4 .^[14] These observations are in line with previous reports and provide conclusive evidence for hypotheses made on the activation of metallocenes with MAO: 1) The observed evolution of methane from metallocene/MAO polymerization systems was proposed by Kaminsky et al.^[15] to be a result of an α -hydrogen transfer reaction of the metallocene $\text{Zr}\text{-Me}$ bonds with those $\text{Al}\text{-Me}$ of MAO, leading to catalytically inactive $\text{Zr}\text{-CH}_2\text{-Al}(\text{Me})\text{-O}$ species; 2) based on limited ^1H NMR spectroscopic data, Britzinger et al. surmised that, upon activation of **1b** with MAO, formation of the putative methylene species $[\text{rac}\text{-}\{\text{Me}_2\text{Si}(\text{-}2\text{-Me-4-Ph-Ind})_2\}\text{Zr}(\mu\text{-CH}_2)(\mu\text{-Me})\text{AlMe}_2]^+$ [$^+\text{Me-MAO}^-$] takes place from the corresponding parent $[\text{rac}\text{-}\{\text{Me}_2\text{Si}(\text{-}2\text{-Me-4-Ph-Ind})_2\}\text{Zr}(\mu\text{-Me})_2\text{AlMe}_2]^+$ [$^+\text{Me-MAO}^-$], accompanied by concomitant evolution of meth-



Scheme 2. Formation and co-crystallization of heterobimetallic **3b** and heterotrimetallic **4b** ($o\text{-F}_2\text{-benzene}$)₂ from $\{\text{SBI}\}$ -based *ansa*-zirconocenium **2b** and AlMe_3 .

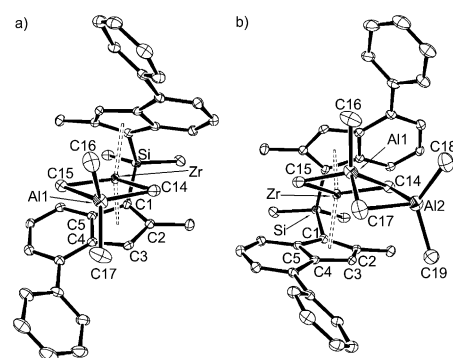
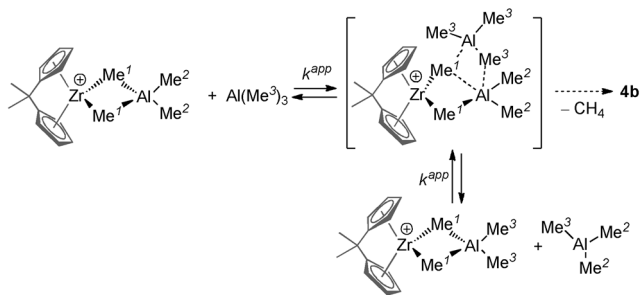


Figure 1. Crystal structures of a) $[\text{rac}\text{-}\{\text{Me}_2\text{Si}(\text{-}2\text{-Me-4-Ph-Ind})_2\}\text{Zr}(\mu\text{-Me})_2\text{AlMe}_2]^+$ (**3b**⁺) and b) $[\text{rac}\text{-}\{\text{Me}_2\text{Si}(\text{-}2\text{-Me-4-Ph-Ind})_2\}\text{Zr}(\mu\text{-CH}_2)(\mu\text{-Me})\text{AlMe}(\mu\text{-Me})(\text{AlMe}_2)_2]^+$ (**4b**⁺). Ellipsoids are set at 50% probability; all hydrogen atoms, $[\text{B}(\text{C}_6\text{F}_5)_4]^-$ anion and molecules of $o\text{-F}_2\text{-benzene}$ are omitted for clarity.^[21]

ane.^[7b,16] This is also reminiscent to Anwender's work on the formation of $\text{Ln}(\mu\text{-CH}_2)\text{Al}$ species via C–H activation of aminomethyl group in neutral lanthanoid alkylaluminum complexes.^[2c]

The molecular solid-state structures of **3b**⁺ and **4b**⁺ are depicted in Figure 1 (selected crystallographic and geometrical parameters are given in the Supporting Information, Tables S1 and S2). Each unit cell of a mixed crystal of **3b**/**4b** ($o\text{-F}_2\text{-benzene}$)₂ contains **3b**⁺ and **4b**⁺ cations with equal populations, two $[\text{B}(\text{C}_6\text{F}_5)_4]^-$ anions and two disordered $o\text{-F}_2\text{-benzene}$ molecules. Although two different molecules **3b** and **4b** are present in the unit cell, the second was modeled using an element of symmetry (center of inversion; see the Supporting Information for details) applied to the first one; thus, the observed atom positions and other geometrical parameters (bond lengths and angles) are virtually the same for both **3b** and **4b**. The geometry of the central $\{\text{Zr}(\mu\text{-Me})_2\text{Al}\}$ bimetallic core in **3b**⁺ (Figure 1a) is similar to that of the slightly dissymmetric Ti/Al analogue in the only structurally characterized AlMe_3 adduct of a titanium post-metallocene.^[8] For instance, the $\text{Zr}\text{-Me}$ bonds are slightly different ($\text{Zr}\text{-C14}$ 2.350(5), $\text{Zr}\text{-C15}$ 2.398(5) Å) while the $\text{Al1}\text{-Me}$ bonds are identical ($\text{Al1}\text{-C14}$ 2.106(5); $\text{Al1}\text{-C15}$ 2.100(5) Å). Also, the latter $\text{Al1}\text{-Me}$ distances in the bridging core are longer than the terminal distances ($\text{Al1}\text{-C16}$ 1.934(6); $\text{Al1}\text{-C17}$ 1.996(6) Å). In the structure of **4b**⁺ (Figure 1b), an additional bridging AlMe_2 moiety is bound with C14H_2 and C17H_3 groups, setting up a new trimetallic $\{\text{Zr}(\mu\text{-CH}_2)(\mu\text{-Me})\text{AlMe}(\mu\text{-Me})\text{AlMe}_2\}$ core. The $\text{Al2}\text{-Me}$ distances ($\text{Al2}\text{-C14}$ 1.934(6); $\text{Al2}\text{-C17}$ 1.996(6) Å) are relatively longer as compared to those of the bimetallic **3b**⁺. The $\text{Al1}\cdots\text{Al2}$ distance in **4b**⁺ (2.576(4) Å) is slightly above the sum of covalent radii of the aluminum atoms and is comparable to $\text{Al}\cdots\text{Al}$ distances observed in the Al_2Me_6 dimer (2.600–2.700 Å).^[17] DFT calculations performed on species **3b**⁺ $[\text{B}(\text{C}_6\text{F}_5)_4]^-$ and **4b**⁺ $[\text{B}(\text{C}_6\text{F}_5)_4]^-$ entirely reproduced the experimental structures of both compounds (see the Supporting Information for details).

The insolubility of crystals of **3b/4b** ($o\text{-F}_2\text{-benzene}$)₂ in toluene, even at elevated temperatures and upon addition of $o\text{-F}_2\text{-benzene}$, hampered their characterization by NMR



Scheme 3. The exchange process of the terminal Me/AlMe₃ groups observed for metallocene AlMe₃ adducts **3a** and **3b**.

spectroscopy. However, satisfactory combustion elemental analysis data were obtained for different, independently prepared batches of these crystals.

The dynamic behavior of AlMe₃ adducts **3a** and **3b** was investigated by ¹H-¹H EXSY spectroscopy on freshly prepared samples at variable temperatures in [D₈]toluene/*o*-F₂-benzene (8:2 v/v) solutions. First, the EXSY spectra recorded for systems of **3a** and **3b** with AlMe₃ at different mixing times (Supporting Information, Figures S10 and S17) revealed rapid exchange between the methyl groups of “free” AlMe₃ and those of the terminal AlMe₂ moieties (Scheme 3). The fact that the rates of this exchange process for both complexes **3a** and **3b** are at least one order of magnitude higher than those for the exchange between “free” AlMe₃ and the bridging methyl {Zr(μ-Me)₂Al} groups (see below) allows a dissociative mechanism involving reformation of the bare ion pairs **2a** and **2b** and “free” AlMe₃ to be discarded.^[5] Moreover, the observed magnetization exchange constants k_{-1}^{obs} and k_{-1}^{obs} for both systems ($k^{\text{app}} = k_{-1}^{\text{obs}}/[\text{AlMe}_3] = k_{-1}^{\text{obs}}/[\text{Zr}]$; see the Supporting Information) depend on the AlMe₃ concentration (provided the monomer/dimer equilibrium for AlMe₃ is very rapidly maintained on the timescale of the methyl group exchange). This suggests that the rate-determining step is the formation of heterotrimeric intermediates (that is, **2a**·(AlMe₃)₂ and **2b**·(AlMe₃)₂) through reversible binding of another molecule of AlMe₃ with **3a** and **3b**, respectively (Scheme 3).^[18] The terminal Me/AlMe₃ groups exchange process appeared to be substantially more facile for {SBI} complex **3b** as compared to that for its {Cp/Flu} analogue **3a**, as evaluated from the rate constants ratio $k^{\text{app}}(\mathbf{3b})/k^{\text{app}}(\mathbf{3a}) = \text{ca. } 140$ at 298 K ([Zr] = 28.0 mM; Table 1). The activation parameters for this exchange process were extracted by a standard Eyring analysis (Supporting Information, Figure S18): **3a** ([Zr] = 28.0 mM, [Al] = 55.0 mM): $\Delta H^\ddagger = 8.5(2) \text{ kcal mol}^{-1}$, $\Delta S^\ddagger = -28(2) \text{ cal mol}^{-1} \text{ K}^{-1}$ and $\Delta G_{298}^\ddagger = 16.70(8) \text{ kcal mol}^{-1}$; **3b** ([Zr] = 10.0 mM, [Al] = 82.0 mM): $\Delta H^\ddagger = 14.95(1) \text{ kcal mol}^{-1}$, $\Delta S^\ddagger = 3.5(1) \text{ cal mol}^{-1} \text{ K}^{-1}$ and $\Delta G_{298}^\ddagger = 13.93(4) \text{ kcal mol}^{-1}$. Although activation entropy values should be compared and discussed with care owing to the uncertainty in their determination,^[19] the substantial difference between such values for the above exchange processes implying **3a** and **3b** likely reflects a significant difference in the nature of the respective heterotrimeric intermediates and the associated transition states.

The two other exchange processes, namely the bridging Me/AlMe₃ exchange and the bridging/terminal methyl groups

Table 1: EXSY-derived apparent rate constants for the terminal Me/AlMe₃ groups exchange process for complexes **3a** and **3b**.^[a]

Complex	[Zr] [mM]	[Al] [mM]	T [K]	Exchange of terminal Me/AlMe ₃ groups	
				k_{-1}^{obs} [s ⁻¹]	$k_{-1}^{\text{app}[b]}$ [M ⁻¹ s ⁻¹]
3a	28.0	55.0	293	0.20(1)	2.8(8)
			298	0.06(1)	
			303	0.19(1)	3.2(3)
			308	0.08(1)	
			298	0.29(2)	4(1)
			308	0.09(1)	
			298	0.42(2)	6(1)
			303	0.13(1)	
			298	0.71(1)	1.9(1)
			303	0.05(1)	
3b	10.0	82.0	278	0.97(2)	2.5(1)
			283	0.07(1)	
			288	5.81(1)	56(15)
			298	0.40(1)	
			283	9.4(3)	85(17)
			288	0.68(1)	
			298	15.9(8)	137(36)
			298	1.0(1)	
			298	39(2)	344(81)
			288	2.6(1)	
3b	28.0	121.0	288	26(1)	175(41)
			298	3.7(1)	173(5) ^[c]
			298	69(3)	447(127)
			298	9(1)	397(8) ^[c]

[a] Determined by ¹H-¹H EXSY NMR spectroscopy in [D₈]toluene/*o*-F₂-benzene (8:2 v/v) solutions. [b] Average value derived from $k^{\text{app}} = k_{-1}^{\text{obs}}/[\text{AlMe}_3] = k_{-1}^{\text{obs}}/[\text{Zr}]$ (see the Supporting Information). [c] Determined from the saturation transfer experiment.

exchange (Supporting Information, Scheme S1), were also observed for **3a** and **3b**; they proceeded, however, with much lower rates (Supporting Information, Table S3) than those observed for the predominant terminal Me/AlMe₃ groups exchange (Table 1).^[20] Again, the observed magnetization exchange constants (k_{-1}^{obs} and k_{-1}^{obs}) for both processes for **3a** and **3b** are dependent on the AlMe₃ concentration; this is consistent with the existence of slow bimolecular processes mediated by formation of heterotrimeric intermediates similar to those proposed for the terminal Me/AlMe₃ group exchange (Scheme 3). Interestingly, only one of the two bridging methyl groups of the {Zr(μ-Me)₂Al} core of **3a** participates in the permutation with AlMe₃ (Supporting Information, Figure S11). This suggests that binding of AlMe₃ with the central heterometallic {Zr(μ-Me)₂Al} core of the C₁-symmetric molecule **3a**, leading to a heterotrimeric adduct and enabling further exchange of methyl groups, exclusively occurs from the more open lateral site (that is, the group opposed to the *t*Bu substituent on the Cp ring).

In summary, we have synthesized and authenticated AlMe₃ adducts of *ansa*-zirconocenes belonging to two different families of highly isoselective propylene polymerization precatalysts, namely, the {Cp/Flu}-based **3a** and {SBI}-based **3b**. Also, we have structurally characterized the first example of a Group 4 metallocene AlMe₃ adduct (**3b**), as well as a product of its decomposition (**4b**), a methylidene species, which results from a C–H activation reaction of one methyl

group after addition of an extra AlMe_3 molecule. Both products nicely co-crystallized in a mixed crystal form **3b/4b**-(*o*-F₂-benzene)₂. The AlMe_3 adducts **3a** and **3b** exhibit in solution a rapid exchange of the terminal methyl groups of AlMe_2 moieties and those of “free” AlMe_3 . This process is two orders of magnitude faster for **3b** as compared to that for **3a** and is apparently mediated by the formation of hetero-trimetallic intermediates (bis(AlMe_3) adducts **2a**-(AlMe_3)₂ and **2b**-(AlMe_3)₂, respectively). These exchange phenomena patterns may be paralleled with the much higher catalytic productivities generally observed for {SBI}-based metallocene systems in olefin polymerization processes as compared to those of their {Cp/Flu}-based congeners: We surmised that the high rate of reorganization of **3b** implying rearrangement of the AlMe_3 ligands in the coordination sphere of zirconium may induce larger amounts of active initiating species. Investigations along these lines are currently under way in our laboratories.

Keywords: aluminum · C–H activation · ion pairs · structure elucidation · zirconocenes

How to cite: *Angew. Chem. Int. Ed.* **2015**, *54*, 6343–6346
Angew. Chem. **2015**, *127*, 6441–6444

- [1] For leading articles, see: a) M. Bochmann, *Organometallics* **2010**, *29*, 4711–4740; b) E. Y.-X. Chen, T. J. Marks, *Chem. Rev.* **2000**, *100*, 1391–1434; c) A. Valente, A. Mortreux, M. Visseaux, P. Zinck, *Chem. Rev.* **2013**, *113*, 3836–3857; d) R. Kempe, *Chem. Eur. J.* **2007**, *13*, 2764–2773.
- [2] a) D. E. Babushkin, H. H. Brintzinger, *J. Am. Chem. Soc.* **2010**, *132*, 452–453; b) M. Van Meurs, G. J. P. Britovsek, V. C. Gibson, S. A. Cohen, *J. Am. Chem. Soc.* **2005**, *127*, 9913–9923. For related neutral lanthanoid-alkylaluminum complexes, see: c) L. N. Jende, C. Maichle-Mossmar, R. Anwander, *Chem. Eur. J.* **2013**, *19*, 16321–16333 and references cited therein.
- [3] Topics in Organometallic Chemistry: U. M. Dzhemilev, V. A. D'yakonov, *Hydro-, Carbo- and Cycloaluminum of Unsaturated Compounds in Modern Organoaluminum Reagents: Preparation, Structure, Reactivity and Use, Vol. 41* (Eds.: S. Woodward, S. Dagorne), Springer, Berlin, New-York, **2013**, p. 215–244.
- [4] M. Bochmann, S. J. Lancaster, *Angew. Chem. Int. Ed. Engl.* **1994**, *33*, 1634–1637; *Angew. Chem.* **1994**, *106*, 1715–1718.
- [5] J. M. Camara, R. A. Petros, J. R. Norton, *J. Am. Chem. Soc.* **2011**, *133*, 5263–5273 and references cited therein.
- [6] J.-N. Pédeutour, K. Radhakrishnan, H. Cramail, A. Defieux, *J. Mol. Catal. A* **2002**, *185*, 119–125 and references cited therein.
- [7] a) D. E. Babushkin, H. H. Brintzinger, *J. Am. Chem. Soc.* **2002**, *124*, 12869–12873 and references cited therein; b) D. E. Babushkin, H. H. Brintzinger, *Chem. Eur. J.* **2007**, *13*, 5294–5299 and references cited therein.
- [8] a) P. D. Bolton, E. Clot, A. R. Cowley, P. Mountford, *Chem. Commun.* **2005**, 3313–3315; b) P. D. Bolton, E. Clot, A. R. Cowley, P. Mountford, *J. Am. Chem. Soc.* **2006**, *128*, 15005–15018.
- [9] For the crystal structure of $[\{\text{SBI}\}\text{Zr}(\mu\text{-H})_3(\text{Al}i\text{Bu}_2)_2]^+ [\text{B}(\text{C}_6\text{F}_5)_4]^-$, see: S. M. Baldwin, J. E. Bercaw, L. M. Henling, M. W. Day, H. H. Brintzinger, *J. Am. Chem. Soc.* **2011**, *133*, 1805–1813.
- [10] a) T. N. Lenton, J. E. Bercaw, V. N. Panchenko, V. A. Zakharov, D. E. Babushkin, I. E. Soshnikov, E. P. Talsi, H. H. Brintzinger, *J. Am. Chem. Soc.* **2013**, *135*, 10710–10719; b) D. E. Babushkin, V. N. Panchenko, H. H. Brintzinger, *Angew. Chem. Int. Ed.* **2014**, *53*, 9645–9649; *Angew. Chem.* **2014**, *126*, 9799–9803.
- [11] AlMe_3 adducts **3a** and **3b** are poorly soluble in neat toluene, and addition of polar *o*-F₂-benzene is required to ensure complete solubility: C. Alonso-Moreno, S. J. Lancaster, C. Zuccaccia, A. Macchioni, M. Bochmann, *J. Am. Chem. Soc.* **2007**, *129*, 9282–9283.
- [12] Compounds **3a** and **3b** were not produced quantitatively if only 1 equiv of AlMe_3 relative to Zr was used. It was originally reported that $[\text{AlMe}_3]/[\text{Zr}]$ ratios of 1.00–1.05:1 are sufficient for complete conversion of ion-pairs $[\text{Cp}_2\text{MMe}]^+ [\text{B}(\text{C}_6\text{F}_5)_4]^-$ into the corresponding adducts $[\text{Cp}_2\text{M}(\mu\text{-Me})_2\text{AlMe}_2]^+ [\text{B}(\text{C}_6\text{F}_5)_4]^-$.^[4] In later studies, however, much larger excess (typically 5–20 equiv of AlMe_3 versus metallocene) was eventually used to quantitatively generate the corresponding AlMe_3 adducts.^[5] In a regular olefin polymerization experiment, co-catalyzed with commercial MAO (containing up to 30 mol % of AlMe_3), $[\text{AlMe}_3]/[\text{M}]$ ratios larger than 50–100 are typically used.
- [13] Owing to the better solubility of metallocenium ion pair **3a**, its concentration can be maintained several times higher than that of **3b**.
- [14] Actual formation of methane in the transformation of **3b** into **4b** was evidenced by ¹H NMR monitoring ($\delta = 0.18$ ppm in $[\text{D}_8]\text{toluene}$) of solutions of **3b** stored over long periods of time at room temperature in sealed NMR tubes. See: a) G. R. Fulmer, A. J. M. Miller, N. H. Sherden, H. E. Gottlieb, A. Nudelman, B. M. Stoltz, J. E. Bercaw, K. I. Goldberg, *Organometallics* **2010**, *29*, 2176–2179; Note that C–H activation and concomitant release of methane can be surprisingly facile in some cationic zirconocenes; see for example: b) M. Bochmann, T. Cuenca, D. T. Hardy, *J. Organomet. Chem.* **1994**, *484*, c10–c12.
- [15] W. Kaminsky, A. Bark, R. Steiger, *J. Mol. Catal.* **1992**, *74*, 109–119.
- [16] This observation also parallels the reactivity reported for $[\text{CpTi}(\text{Me})_2(\text{N}=\text{PR}_3)]$ complexes with respect to AlMe_3 ; J. E. Kickham, F. Guerin, J. C. Stewart, D. W. Stephan, *Angew. Chem. Int. Ed.* **2000**, *39*, 3263–3266; *Angew. Chem.* **2000**, *112*, 3406–3409.
- [17] a) R. G. Vranka, L. A. Elmer, *J. Am. Chem. Soc.* **1967**, *89*, 3121–3126; b) G. S. Mcgrady, J. F. C. Turner, R. M. Ibberson, M. Prager, *Organometallics* **2000**, *19*, 4398–4401.
- [18] S. Lieber, M.-H. Proscenc, H. H. Brintzinger, *Organometallics* **2000**, *19*, 377–387.
- [19] P. J. Barrie, *Phys. Chem. Chem. Phys.* **2012**, *14*, 327–336 and references cited therein.
- [20] It should be mentioned that, owing to the very different kinetic regimes for these three exchange processes, that is, quite slow for the bridging Me/ AlMe_3 groups and the bridging/terminal methyl groups exchanges and quite fast for the terminal Me/ AlMe_3 groups exchange, although all were monitored at the same time using a constant mixing time (experimental constraint), there is an inaccuracy in the determination of the corresponding rate constants for the two former processes. Therefore, the corresponding rates and thermodynamic parameters (ΔH^\ddagger , ΔS^\ddagger , and ΔG_{298}^\ddagger) extracted for the two former processes (Supporting Information, Figure S20) should be used and compared with care.
- [21] CCDC 1051621 (**3b/4b**-(*o*-F₂-benzene)₂) contains the supplementary crystallographic data for this paper. These data can be obtained free of charge from The Cambridge Crystallographic Data Centre via www.ccdc.cam.ac.uk/data_request/cif.

Received: March 2, 2015

Published online: April 7, 2015